

Article

Powdered Activated Carbon Exacerbates Fouling in MBR Treating Olive Mill Wastewater

Noya Ran , Jack Gilron, Revital Sharon-Gojman and Moshe Herzberg * 

Zuckerberg Institute for Water Research, The Jacob Blaustein Institutes for Desert Research, Ben-Gurion University of the Negev, Sede Boqer Campus, Midreshet Ben-Gurion 84990, Israel; noyar@post.bgu.ac.il (N.R.); jgilron@bgu.ac.il (J.G.); sharre@exchange.bgu.ac.il (R.S.-G.)

* Correspondence: herzberg@bgu.ac.il; Tel.: +972-8-6563520

Received: 7 October 2019; Accepted: 25 November 2019; Published: 27 November 2019



Abstract: Membrane fouling is a major obstacle in membrane bioreactors (MBRs) that treat wastewater. The addition of powdered activated carbon (PAC) is commonly suggested as a way to improve the MBR wastewater treatment process with respect to membrane fouling and effluent quality. Integrating the PAC addition into the MBR may also improve the stability of the acclimated microbial community for biodegrading the recalcitrant organic compounds that can also enhance membrane fouling. In this study, the ability of the MBR-PAC system to decrease membrane fouling was evaluated. Two pilot-scale reactors were operated: one reactor was supplemented with suspended PAC, and one was operated under similar conditions, without PAC. The feed to the reactors comprised domestic and olive oil mill wastewater. Surprisingly, the permeate flux and the membrane permeability decreased faster in the MBR supplemented with PAC compared to the control reactor. Corroborating these MBR fouling results, soluble microbial products (SMPs), originating from the PAC-supplemented reactor, were found to be more adhesive to an ultrafiltration membrane mimetic surface (polyether sulfone) as analyzed in a quartz crystal microbalance with dissipation monitoring (QCM-D). While the PAC had almost no effect on the dissolved organic carbon in the MBR, it altered the molecular weight distribution of the organic molecules in the SMP as observed with gel permeation chromatography: The fractions of 577–789 kDa and the one bigger than 4×10^3 kDa, were elevated and reduced, respectively, by the addition of PAC. A biofilm formation analysis using a confocal laser scanning microscopy showed a higher amount of biofilm on the membrane taken from the PAC reactor, but this membrane showed no traces of PAC particles when analyzed with a scanning electron microscope (SEM). Taken together, altering the composition of the dissolved organic matter in the MBR by PAC addition promoted its adhesion to the membrane, induced biofilm formation, and more prominently, decreased membrane permeability.

Keywords: powdered activated carbon; membrane bioreactor; QCM-D; fouling; biofouling

1. Introduction

Membrane bioreactor (MBR) technology combines the microbial degradation of organic compounds and membrane separation [1]. Due to water scarcity in densely populated areas and a decrease in the operational cost of submerged membrane reactor configurations, the use of this technology is expanding and providing an alternative to the conventional activated sludge (AS) process [2]. The MBR's ability to de-couple the hydraulic retention time (HRT) and the solids retention time (SRT), retaining bacteria, viruses and even large molecules in the reactor for longer time periods, makes this technology advantageous over AS processes [3]. Optimal membrane performance is commonly indicated by achieving the lowest transmembrane pressure (TMP) under constant flux conditions or the highest flux under a constant TMP [4]. Membrane fouling includes organic, colloidal,

inorganic and microbial fouling (biofouling) and therefore, represents a major challenge to MBR operations [5].

The proliferation of microorganisms on the membrane commonly degrades membrane performance, as expressed by elevated specific energy consumption and more frequent backwash and chemical cleanings. An increased membrane cleaning frequency is required since the microorganisms survive even under stressed conditions, such as backwashing with different chemicals [6]. Several biofouling processes in ultrafiltration (UF) membranes in MBRs have been examined, including (i) adsorption of extracellular polymeric substances (EPS) to the membrane surface and pores, (ii) clogging of the membrane pores by colloidal particles or by soluble microbial products (SMP) originating from the MBR's microorganisms, and (iii) deposition of cells and biofilm formation on the membrane surface [7].

The application of activated carbon (AC) in bioreactors degrading organic compounds provides two possible advantages: AC can adsorb biodegradable compounds that have a low molecular weight from contaminated water and during this adsorption process, microorganisms can colonize its outer surface. Such microbial activity on the AC is commonly termed biological activated carbon (BAC), creating conditions of adsorption/desorption and continuous biodegradation, which elevate the microbial activity in the bioreactor due to the larger biomass surface area exposed to the substrate [8,9]. In addition, the sessile microorganisms on the AC are physically protected by the AC's rough surface, and the presence of a large variety of functional groups on the surface of the carbon enhances the adhesion of the microorganisms. As a result, sessile microorganisms on AC were found to be highly resistant to disinfectants [10]. The functioning of an MBR loaded with powdered activated carbon (PAC) [11] was previously investigated for its ability to: (i) improve the stability of the microbial communities by providing a favorable surface for the creation of flocs [10], (ii) buffer the microbial response to sudden elevation in the organic matter in the feed, (iii) increase removal of micro-pollutants [12,13], and (iv) reduce the fouling propensity of the membrane, observed as an elevation in the critical flux [14]. Reduced membrane fouling was attributed to the adsorption of certain organic compounds present in the EPS of flocs, as well as in the SMP dissolved in the MBR's mixed liquor [15–19]. It was proposed that such adsorption of SMP components to the PAC changed the SMP composition (protein to carbohydrate ratio) [10].

Olive oil mill wastewater (OMWW) is the effluent produced during the olive oil production process. This wastewater is a dark reddish-black, mildly acidic liquid of high conductivity, with high levels of organic matter. Its chemical oxygen demand can be higher than 200 g/L, and its biological oxygen demand can be higher than 100 g/L [20]. Another OMWW characteristic is its high content of phenol compounds, whose concentrations vary from 0.5 to 24 g/L [21]. The treatment and disposal of OMWW are currently one of the most serious environmental problems in the olive oil production process, due to the large quantities of waste that are generated in short periods of time. So far, the methods tested for treating OMWW have included thermal concentration [22], treatment with lime [23], physicochemical processes such as oxidation by Fenton's reagent [24] or electrocoagulation [25,26], biological treatments [27–29] and membrane processes [27–33].

The application of MBR technology for industrial wastewater treatment is common because of the robustness of the process, its ability to endure high organic loadings, and its high specificity for certain microbial communities in the degradation of unique refractory substrates [34,35]. Therefore, MBR has also been studied for treating OMWW [35]. The addition of AC to an MBR can decrease the phenol's toxicity and, therefore, may improve the overall biodegradation efficiency of the system. Importantly, the adsorption of potential organic foulants by the AC may lead to a reduction in the membrane's organic fouling and biofouling in the MBR, as noted above. Hence, the MBR-PAC system seems an excellent choice for OMWW treatment. In this study, we examine the hypothesis that the PAC supplement will indeed improve MBR performance. This hypothesis is based on the assumption that PAC serves as an alternative medium to the membrane surface for the adsorption of organic foulants. As such, the presence of PAC may sequester organic fouling and any consequent biofouling by reducing

the amount of organic matter conditioning the membrane. To study the effect of PAC addition to the MBR, we utilized adsorption tests in a quartz crystal microbalance with dissipation monitoring (QCM-D) with SMP originating in the pilot-scale MBR with and w/o PAC. The QCM-D enables real-time observation of interactions of colloids and dissolved organic matter with surfaces [36], which quantify both adhesion and the layer's viscoelastic properties. The adherence of SMP to the membrane mimetic surface, a polyether sulfone (PES)-coated QCM-D surface, was analyzed in parallel with dead-end filtration tests in order to isolate the PAC effects on the adsorption of dissolved organic compounds to the membrane and eventually, on changes in the membrane permeability. The accumulation of fouling layers and possible changes in the SMP composition were also analyzed and related to the presence of PAC and its effects on membrane fouling.

2. Materials and Methods

2.1. MBR System and Operating Conditions

Two MBRs, equipped with a submerged UF membrane module of microdyn-nadir® (Wiesbaden, Germany), were operated. The flat sheet membrane (UP150) module configuration comprised a PES membrane, with a mean pore size of 0.04 μm (MWCO of 150 kDa) and a total effective filtering surface area of 0.34 m^2 . The bioreactor's volume was ~ 90 L. The initial and constant concentration of the PAC in the MBR-PAC system was 0.1 g/L (Sigma C-33454). The average particle size of the PAC was 100–400 mesh (37–149 μm). The filtration pumping cycle in the MBR was 4.5 min of filtration and 30 sec of backwash. The initial flow rate was ~ 30 ml/min corresponding to an initial flux of ~ 5 LMH, and the initial transmembrane pressure was ~ 0.065 mBar, in both reactors. The reactors were fed with OMWW that was collected from an industrial olive mill press near Rahat, a city in Israel's Negev region, together with domestic wastewater that originated from Ben-Gurion University's student dormitories (2:1 ratio) (the mix of the two effluents provided $\sim 20,000$ mg/L of dissolved organic carbon (DOC) and 17,000–44,000 mg/L of biological oxygen demand (BOD)). Each day, 3 L of sludge was removed, providing a 30-d SRT. A proper amount of PAC was added each day to maintain 0.1 g/L of PAC in the MBR-PAC system. Preliminary experiments with a higher dosage of PAC (1 g/L) were performed in order to avoid possible fouling by PAC particles (Figure S5, supplementary information).

Aeration was provided by an air diffuser at the bottom of the reactor to provide oxygen for the biomass, to maintain good mixing and homogeneity of the mixed liquor suspended solids (MLSS), and to remove biomass flocs and organic material from the membrane surface. The permeate flux was measured volumetrically, and TMP was monitored by a pressure gauge, as well as by a digital indicator. The SMP sample was extracted from the MLSS of the reactor by centrifugation at 3500 g and filtration through a 0.45- μm hydrophilic membrane (PALL Supor 200, 47 mm, Port Washington, NY, USA). The MBR fouling experiments were conducted in duplicate, each time with a different UF membrane module. The MBR's mean operational temperature of 24.0 ± 1.4 °C was maintained by a thermostatted heater submerged in the MLSS. Dissolved oxygen (DO) was monitored by an oxygen meter (Model 550, YSI, Yellow Springs, OH, USA). The continuous flow of feed wastewater was regulated by a level-control valve. The operating conditions and the influent and effluent characteristics of the duplicated MBR runs are presented in Tables 1 and 2, respectively.

Table 1. Conditions of the membrane bioreactors (MBRs).

Parameter	Run A		Run B	
	PAC	Control	PAC	Control
DO (mg/L)	0.5 ± 0.2	0.7 ± 0.2	0.2 ± 0.0	0.3 ± 0.0
pH	6.5 ± 0.2	6.3 ± 0.2	6.7 ± 0.1	5.5 ± 0.05
Volatile suspended solids (VSS, g/L)	3.3 ± 0.4	4.5 ± 0.8	3.7 ± 0.6	6.7 ± 1.5
Temperature °C	23.4 ± 0.4	23.5 ± 0.6	24.8 ± 0.9	24.0 ± 0.3
Volumetric organic loading rate (g/(h·l))	0.74 ± 0.1	0.66 ± 0.02	0.27 ± 0.07	0.28 ± 0.05
Specific BOD removal rate (g/(h·gVSS))	0.18 ± 0.03	0.12 ± 0.03	0.06 ± 0.02	0.01 ± 0.00
Specific DOC removal rate (g/(h·gVSS))	0.07 ± 0.02	0.06 ± 0.01	0.05 ± 0.02	0.03 ± 0.01

Table 2. Influent and effluent characteristics of the MBRs.

Run A										
Parameter	PAC					Control				
	Influent	MLSS	Effluent	Biodegradation (%)	Overall removal (%)	Influent	MLSS	Effluent	Biodegradation (%)	Overall removal (%)
BOD (g/L)	44 ± 0.0	8.1 ± 0.2	7.4 ± 0.4	81.6 ± 2.0	83.2 ± 4.5	35 ± 0.1	5.1 ± 0.7	5.8 ± 0.4	85.4 ± 11.7	83.4 ± 5.7
DOC (g/L)	21 ± 0.9	6.7 ± 1.7	5.8 ± 1.9	68.1 ± 17.5	72.4 ± 23.9	20 ± 1.2	5.6 ± 0.5	5.0 ± 0.2	72.0 ± 7.7	75 ± 5.4
Phenol content (g/L as gallic acid)	0.8 ± 0.2	0.5 ± 0.1	0.4 ± 0.1	37.5 ± 12.0	50 ± 17.7	0.6 ± 0.1	0.4 ± 0.1	0.4 ± 0.0	33.3 ± 10.0	33.3 ± 5.5
Run B										
	PAC					Control				
BOD (g/L)	21 ± 0.8	6.1 ± 0.0	5.7 ± 0.5	71.0 ± 2.7	72.8 ± 7.0	17 ± 1.4	11.3 ± 0.7	8.7 ± 0.4	33.5 ± 3.5	48.8 ± 13.0
DOC (g/L)	19 ± 2.1	6.3 ± 0.7	5.7 ± 1.1	66.8 ± 10.5	70.0 ± 15	19 ± 1.7	6.2 ± 1.3	5.6 ± 0.9	67.4 ± 15.4	70.5 ± 13.0
Phenol content (g/L as gallic acid)	0.7 ± 0.2	0.7 ± 0.0	0.6 ± 0.1	0.0 ± 0.0	14.3 ± 4.7	0.8 ± 0.1	0.5 ± 0.1	0.5 ± 0.1	37.5 ± 8.8	37.5 ± 8.8

2.2. Fouling Rate Analysis with SMP and Membrane Permeability Tests

The UF test unit comprised a dead-end cell hosting a membrane with a circle-shaped channel holder (radius = 2.2 cm), a peristaltic pump, an electronic balance, and a data-acquisition system (PC-interfaced) that was used to acquire the pressure and the accumulated permeate (Figure 1). The system was operated in a closed-loop mode with the feed solution recirculated into the reservoir. A commercial UF membrane (UP150 Microdyn Nadir, Wiesbaden, Germany) was used in the filtration unit as a model membrane for the fouling experiments. The membrane, which was received as a flat sheet, was cut into circles with radii of 2.2 cm. The DI water permeability was measured and calculated at four different pressures (between 0.3 and 0.7 bar), followed by an hour of fouling with SMP extracted at the end of the second duplicate MBR run, at an initial pressure of 0.6 bar. Then, the DI water permeability was again measured in the same range of four different pressures (between 0.3 and 0.7 bar).

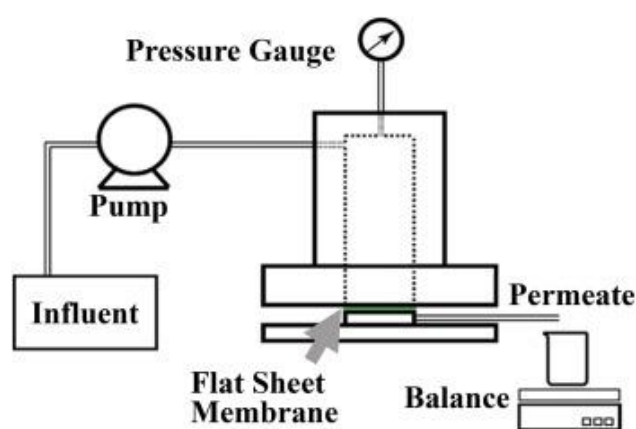


Figure 1. A schematic diagram of an ultrafiltration (UF) dead-end filtration unit.

2.3. QCM-D Sensor Preparation and Coating with PES for SMP and EPS Adhesion Measurements

All the QCM-D sensors (Q-Sense, Biolin Scientific, Gothenburg, Sweden), AT-cut gold-coated quartz crystals, were mounted for the adhesion/fouling experiments, in E4 modules. The QCM-D sensors were spin-coated with PES according to the following protocol: Prior to the coating procedure, the gold-coated quartz crystals were thoroughly cleaned by exposure to UV radiation for 10 min and then submersion for 5 min in a 5:1:1 mixture of DI, 25% ammonia, and 30% hydrogen peroxide at 75 °C, followed by washing with N-Methyl-2-pyrrolidone (NMP). Then, the sensors were washed with DI water, dried with 99.99% pure nitrogen to remove moisture and accumulated dust particles, and finally, exposed to UV radiation for 10 min in an ozone chamber (BioFORCE Nanoscience, Ames, IA, USA). Spin-coating was performed with 65 μ l of 1% PES (w/v) in dichloromethane, filtered through a PVDF 0.22- μ m syringe filter (Millipore, Rosh-Ha'ayin, Israel). The PES solution was placed in the midpoint of the sensor immediately prior to spinning at 2700 revolutions per second for 1 min. PES surface coating was verified with ATR-FTIR and contact angle analyses.

2.4. SMP Adherence Property Analysis with QCM-D

The modified PES-coated sensors were used for the SMP adsorption experiments. For these experiments, samples of SMP were collected at the end of the MBR runs and injected in the following sequential stages: DI water for 45 min, background solution for 45 min (17 mM NaCl with 1 mM CaCl₂), SMP (20 mg/L as DOC) dissolved in the background solution for 90 min, background solution for 45 min, and finally, DI water for 45 min. All experiments were conducted at 25 °C. The magnitude of SMP adsorption to the QCM-D sensors was defined by the change in the oscillation frequency shift at the end of the following two stages: (i) the absolute frequency shift prior to SMP addition (after

baseline with background solution, without SMP), and (ii) the absolute frequency shift after SMP adsorption and washing with the background solution.

2.5. Confocal Laser Scanning Microscopy (CLSM)

After the first MBR run, the membrane modules were removed from the reactor, cut into pieces of approximately 1 cm^2 and fixed immediately, without drying the sample. The fixation was performed by placing the sample in a solution of 0.85% NaCl and 2% glutaraldehyde for 1 h. Then, samples were stained with concanavalin A (ConA) conjugated to Alexa Fluor 633 (Invitrogen, Rehovot, Israel) and propidium iodide (PI) for probing EPS and cells, respectively. Microscopic observation and image acquisition were performed using a Zeiss-Meta 510 (Jena, Germany), a CLSM equipped with a Zeiss dry objective LCI Plan-Neo Fluor (20x magnification and a numerical aperture of 0.5). The CLSM images were generated using the Zeiss LSM Image Browser. Images were analyzed, and the specific biovolume ($\mu\text{m}^3 \cdot \mu\text{m}^{-2}$) and the average thickness (μm) in the biofouling layer were determined using the COMSTAT software [37] written as a script in Matlab 6.5 (The Math Works, Inc., Natick, MA, USA) and equipped with an image-processing toolbox. For every sample, six positions on the membrane were chosen and microscopically observed, acquired, and analyzed. A three-dimensional reconstruction of the CLSM image stacks was carried out using Imaris software (Imaris Bitplane, Zurich, Switzerland).

2.6. Scanning Electron Microscopy (SEM)

An analysis of the membrane surface structure and the morphology of the fouled membrane samples was conducted using an ESEM (FEI Company, Philips XL30, Oregon, USA) (resolution 6 nm) equipped with an EDX-Genesis 4000 energy dispersive X-ray fluorescence spectrometer. The measurements were done in a conventional high vacuum mode for imaging of the fouling layers. Prior to the measurement, the fouled membrane layers were fixed, dehydrated, and coated with a layer of carbon with an approximate thickness of 10–15 nm. The fixation method included the following steps: (1) The excess electrolyte solution was carefully removed with a filter paper from the specimens (fouled membrane pieces of around $1\text{ cm} \times 1\text{ cm}$). (2) The fouled membrane specimens were incubated in a 0.05 M sodium cacodylate buffer supplemented with 2% glutaraldehyde (Electron Microscopy Sciences, Fisher Scientific) for 1 h. (3) The specimens were incubated for 10 min and rinsed three times with a 0.05 M sodium cacodylate buffer. (4) A second fixation step was performed by incubating the specimens in a 0.05 M sodium cacodylate buffer supplemented with 1% osmium tetroxide for 1 h (Electron Microscopy Sciences, Fisher Scientific). (5) Excess amounts of osmium tetroxide were removed according to the same procedure followed in step 3. (6) Specimens were dehydrated during a 20-min incubation period each in ethanol/water solutions with increasing ethanol concentrations (25, 50, 75, 95, and 100%). (7) Finally, the specimens were washed once with hexamethyldisilazine (Electron Microscopy Sciences, Fisher Scientific) and dried overnight in a hood at room temperature.

2.7. Gel Permeation Chromatography (GPC)

The GPC analysis was performed with the ACQUITY APC system (Waters Co., Milford, MA, USA) and 20% methanol in double-distilled water (DDW), as the eluent. Samples were dissolved in DDW. All samples and standards were eluted as indicated by the UV detector absorption response peak (254 nm) and a combination of $3 \times$ Ultrahydrogel TM columns, 1000, 250, and 120: $7.8 \times 300\text{ mm}$. Poly(styrene sulfonates) standards (Waters Co., Milford, MA, USA) were used for the UV calibration with the following molecular weights: 976 kDa, 470 kDa, 258 kDa, 78.4 kDa, 29.5 kDa, 10.2 kDa, 4.20 kDa, 1.67 kDa, 0.89 kDa, and 0.20 kDa. The standards were freshly produced and measured within 2 d. Then 1 mg/mL of the standards and samples was dissolved in deionized water and filtered through $0.2\text{-}\mu\text{m}$ filters (Thermo Fisher, PA, USA) prior to the GPC analysis. The samples' injected volume was $50\text{ }\mu\text{L}$, and the mobile phase flow rate was 0.5 mL/min at $45\text{ }^\circ\text{C}$ for 70 min. The data analysis was performed using Waters Empower software.

3. Results and Discussion

3.1. The Effect of Supplementing MBR with PAC on Membrane Fouling

The effect of the PAC addition to the MBR on membrane fouling was tested under a constant dosage of 0.1 g/L PAC to the MBR. Figure 2a,b shows the variations of membrane permeability over time, during the two fouling experiments in the MBRs. In both experiments, the initial permeability values in both reactors were similar (~80 LMH/bar for the first experiment and ~63 LMH/bar for the second experiment). Surprisingly, the addition of PAC to the MLSS in the MBR reduced the membrane permeability to less than 25% of the membrane permeability in the MBR without PAC addition (Figure 2a,b). It should be mentioned that the reduced permeate flux of the MBRs was affecting their refill rate by a water-level controlled valve fed with municipal wastewater with much lower DOC and BOD concentration than values of the OMWW feed to the MBRs. Therefore the PAC supplemented MBR, was eventually being fed with slightly higher average values of BOD and DOC in the feed solution (Table 2) than the control reactor. The MLSS and effluent quality (BOD and DOC) in the PAC reactor were close to the control reactor (slightly higher in Run A and slightly lower in Run B (Table 2)). For the case of PAC addition, as expected and reported in previous work [11–13], the specific biodegradation rate of the PAC reactor was higher in both runs with respect to DOC and BOD biological removal (Table 1). Under such conditions, in which the PAC reactor performance was close to the control reactor and stabilized with lower VSS concentration (Table 1), we aimed at understanding the unexpected exacerbated fouling in MBR fed with PAC. Five possible reasons could explain the extreme reduction in membrane permeability for the case in which PAC was supplemented to the reactors: (i) selective adsorption by the PAC of certain organic components that are less prone to adsorb to the membrane, while in parallel, elevation in the relative concentration of organic compounds with a higher affinity for the membrane, (ii) membrane pore blockage by the PAC particles, (iii) induced biofilm growth on the membrane surface as a result of removal by the PAC of certain compounds toxic to the microorganisms, (iv) changes in the SMP composition due to changes in specific biomass activity caused by PAC addition, and (v) changes in the microbial communities, which enhance membrane biofouling, attributed to PAC addition. To examine possible SMP effects on membrane fouling, dead-end permeability experiments with SMP samples collected from the reactors, as well as adsorption experiments of the SMP to PES-coated QCM-D sensors, were conducted.

The SMP samples collected from the two reactors, with and w/o PAC, were used for membrane fouling experiments, in order to determine the fouling propensity of the dissolved organic matter and the potential related impact of PAC addition. Following a dead-end filtration of the SMP solutions (50 ± 3.0 mg/L as DOC dissolved in deionized water) and backwash through the PES UF membranes, similar to the one placed in the submerged module in the MBR, the DI water permeability was measured. This procedure allowed the assessment of the irreversible fouling caused by adsorption of SMP to the membrane pores. Note that the amounts of total organic content in the two different SMP samples collected from the two reactors were similar. The values of the initial flux were 5.12 and 5.72 LMH for the PAC and control samples, respectively, values that are similar enough to eliminate the possibility of initial flux effects on the fouling propensity. The values of the initial permeability were 16.8 ± 0.92 and 15.0 ± 1.86 LMH·bar⁻¹ for the PAC and control experiments, respectively. The values of the irreversible permeability loss (irreversibly reduced permeability, which was not recovered by the backwash step) were 9.3 and 6.0 LMH·bar⁻¹ for the PAC and control samples, respectively. Flux decline pattern and permeability loss of the membranes used for the dead-end filtration experiments are shown in the Supplementary Information, Figure S1. It should be mentioned that the SMP sample used in this procedure was free of PAC particles (0.45 µm filtered). Hence, the greater decrease in membrane permeability for the SMP of the PAC reactor could be explained by a certain change in the SMP composition attributed to the addition of PAC to the reactor. While DOC concentration was similar in both reactors, it seems that the PAC reactor contained higher concentrations of adhesive compounds.

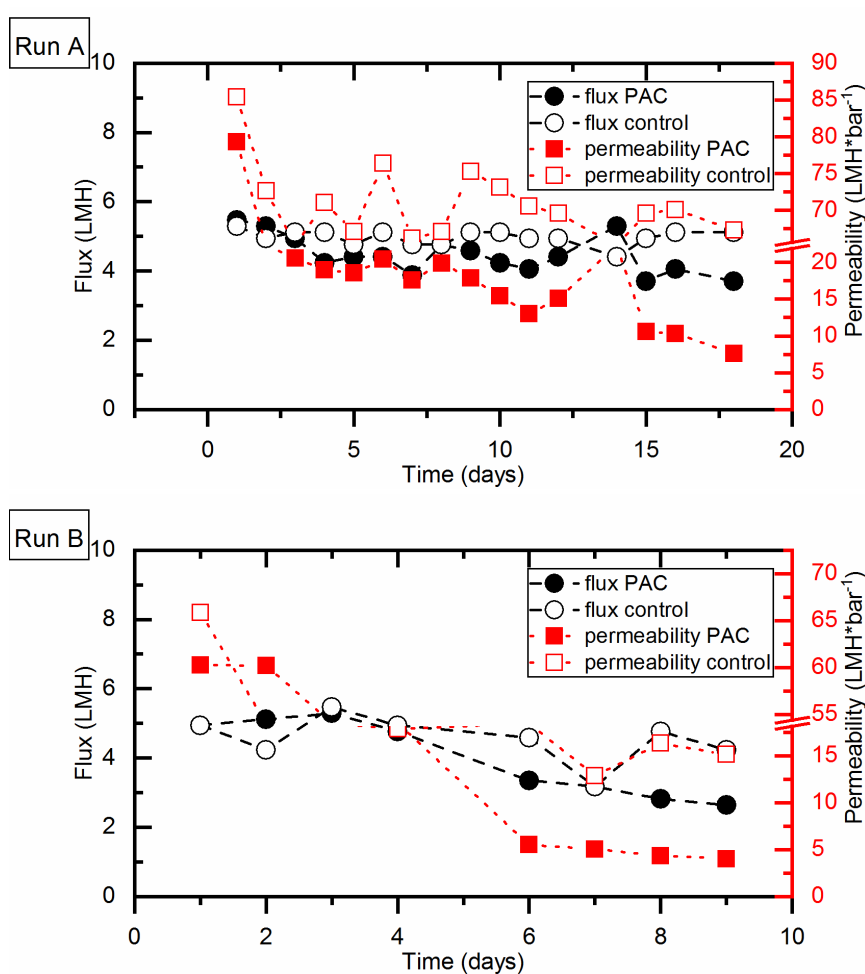


Figure 2. The effects of powdered activated carbon (PAC) addition on the decrease in permeate flux and permeability in the MBRs. **Run A:** Average Flux PAC— 4.5 ± 0.6 LMH Control 5.0 ± 0.2 ; **Run B:** Average Flux PAC— 4.0 ± 1.1 Control 4.5 ± 0.7 LMH.

3.2. The Effect of Supplementing an MBR with PAC on the SMP Adherence Properties

In order to define the adsorption tendency and adhesiveness of the dissolved organic matter in the SMP originating from the reactors, adsorption experiments on membrane mimetic surfaces were performed on QCM-D sensors. The PES-coated QCM-D sensors were used to mimic the active layer of the membrane, and SMP samples, collected from the MBRs, were injected in continuous flow on top of the coated sensors. Figure 3 Run A and B provide the oscillation frequency shifts of the PES-coated sensors measured during three different stages of the adsorption experiment. At the first stage, the injected background solution provides a small frequency shift (comparing to a baseline with deionized water) attributed mainly to the change in the viscosity of the boundary layer in close proximity to the sensor. In the second stage, when the SMP sample is injected, the decrease of the frequency shift is attributed to the adsorption of dissolved organics from the sample to the sensor's surface. During the third stage of the experiment, a background solution is injected and removes organic matter reversibly adsorbed to the sensor, causing its desorption and consequent elevation of the frequency shift. As shown in Figure 3 Run A higher reduction in the frequency shift was observed for the adsorbed organic matter of the sample obtained from the PAC reactor compared to the control reactor (~ 30 Hz vs. ~ 25 Hz). The second adsorption experiment (Figure 3 Run B) showed the same trend. The decrease in the frequency shift by the SMP of the PAC reactor was higher than the one of the control reactors (~ 22 Hz vs. ~ 17 Hz, respectively). The adhesion of SMP, originating from the MBRs to PES-coated sensors verifies the higher fouling propensity of the dissolved organic

compounds in the PAC reactor. The elevated adsorption of organic matter from the PAC-supplemented MBR corroborates both (i) the elevated fouling rate observed in the PAC reactor, and (ii) the lower permeability of the UF membrane exposed to the SMP of the PAC reactor after the dead-end fouling experiments. Since in both reactors, no significant difference in the DOC concentrations of the MLSS was detected and in addition, all samples were tuned to similar DOC concentrations, it seems that the PAC reactor selected for certain organic compounds with higher affinities for the membrane, in which the involved mechanism is unknown and thorough characterization of the organic matter is required. Interestingly, EPS, which was extracted from the MLSS [36–38] of the two reactors did not show clear difference in its affinity to the PES coated QCM-D sensors: in one case, higher adsorption rate was detected for the EPS of the control reactor, and in another case, no change was detected (Supplementary Information, Figure S2). This result might be attributed to the notion that the exposure of the influent wastewater to the microorganisms with PAC, had no effect on the adherence of the extracellular matrix to the membrane and rather, changes in the SMP composition had further effects on the consequent membrane fouling and biofilm formation.

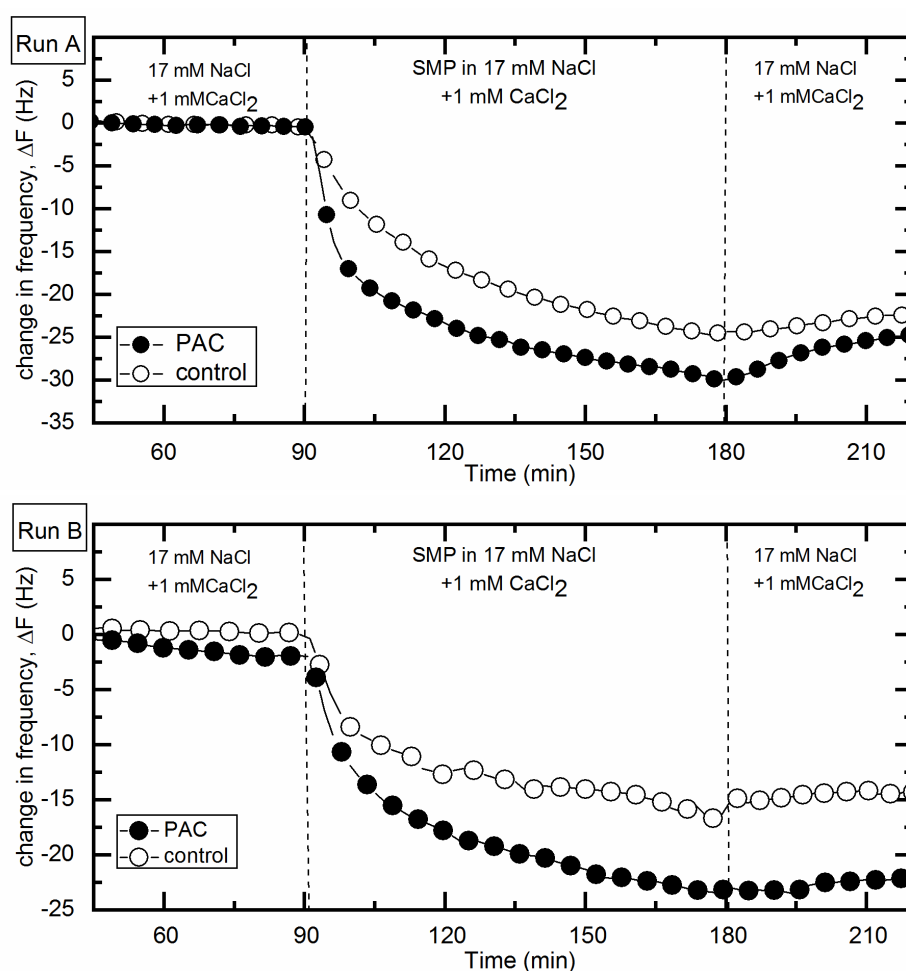


Figure 3. The effect of PAC addition to the MBRs on the adherence properties of the soluble microbial products (SMPs): Two replicates of QCM-D adhesion profiles of the SMP, extracted from the MBR (Run A and Run B), provided as frequency shifts during SMP adhesion to PES-coated sensors at the ninth overtone. A background solution with an ionic strength of 20 mM (17 mM NaCl ± 1 mM CaCl₂) was supplemented with SMP (20 mg/L ± 1.7 as dissolved organic carbon (DOC)) collected from two runs (Run a and Run b).

3.3. The Effect of Supplementing an MBR with PAC on SMP Composition

In order to examine the assumption that PAC alters the SMP composition so that it will have a higher affinity for the membrane, the size distribution of the organic molecules constituting the SMP was analyzed by GPC (Figure 4). The SMP samples were collected at the end of the second MBR run (Figure 2b), and interestingly, the GPC chromatograms showed a distinct difference between the control and the PAC-supplemented reactors. The first peak of the SMP from the control reactor at a retention time of 24 min was significantly reduced in the SMP of the PAC reactor, while a rise in the peak at 28 min was observed in the SMP of the PAC reactor (Figure 4, peaks a and b, respectively). A peak at 37 min was also elevated in the SMP of the PAC reactor (peak c). Changes in the amount of certain organic compounds (elevation or reduction) in the SMP could be attributed either to (i) increased production and secretion of certain microbial products as a result of changes in the microbial community composition or enhanced metabolic activity as observed for PAC addition, or (ii) inhibition in the degradation of material in the influent wastewater. The adsorption of organic compounds to PAC particles can only decrease their appearance in the SMP. As already mentioned, the PAC SMP provided higher adhesion of organic matter to a membrane mimetic surface, as well as a higher fouling rate, in both the dead-end filtration experiments and the MBR plant. It is also possible that the reduction in certain components in the SMP (such as seen in peak a), due to adsorption to the PAC, provides preferential adsorption of other components that are more detrimental to flux reduction or that function as membrane conditioning precursors, which may enhance biofilm growth (such as peaks b–d). Clearly, determining the identity of the organic foulants on the membrane is an essential task, and for now, the detailed effects of the different SMP components on membrane fouling as well as their adsorption to PAC are unknown.

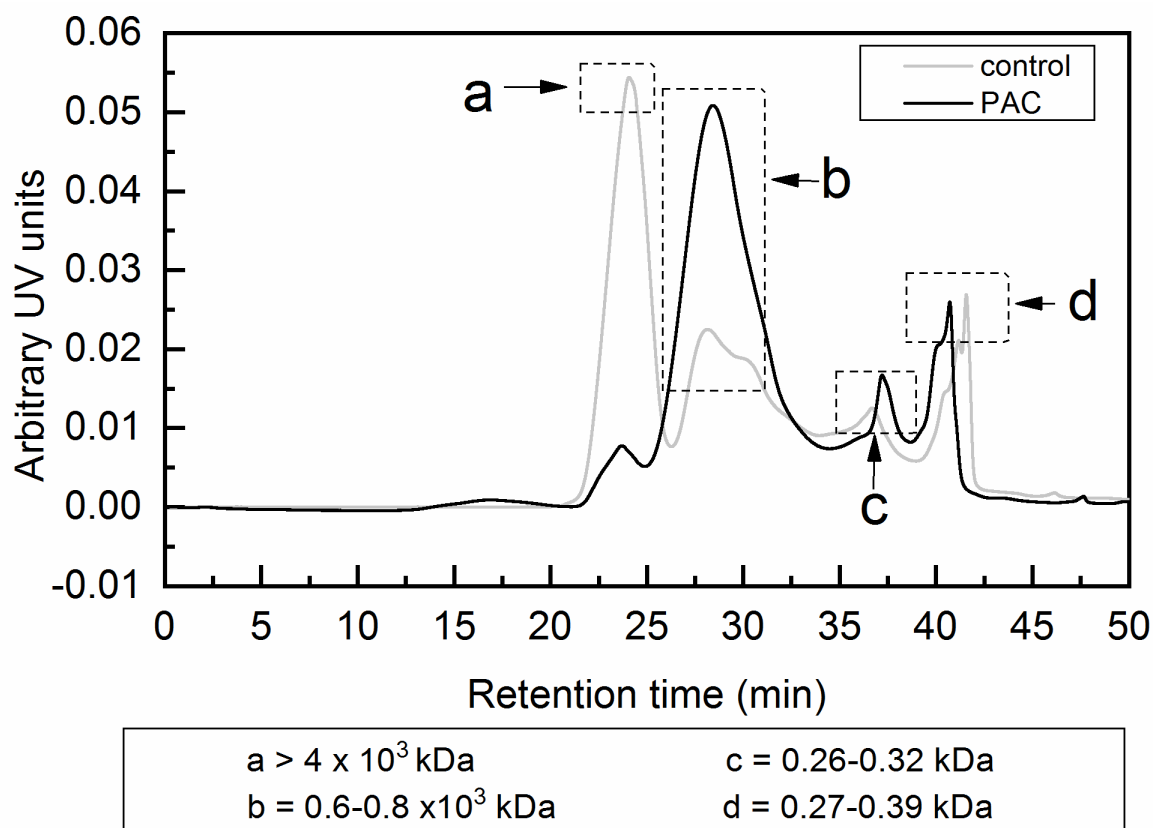


Figure 4. The effect of PAC addition to the MBRs on the SMP composition: gel permeation chromatography (GPC) chromatograms of SMP collected from the second run: The peak (a) > 4 × 10³ kDa is reduced versus the elevation of the peak (b) of the 577–789 kDa organic molecules. The GPC mobile phase was a 20% methanol solution in DI water.

3.4. Variation in Biofilm Formation with PAC Addition

In order to analyze the possibility of elevated biofilm formation due to PAC addition to the MBR and to further elucidate the cause for the higher magnitude in the decrease in membrane performance in the PAC reactor, membrane autopsies were carried out at the end of the first MBR run (Figure 5A,B). In comparing the nature of the biofilm structure between the two reactors, it is observed that the elevated flux decline of the PAC reactors is clearly related to the magnitude of biofilm growth. CLSM analyses of biofilms on the two membranes, taken from the modules at the end of the first MBR run, show a significant difference in the biovolumes of the cells and their self-associated EPS between the PAC and the control reactors (Figure 5C,D). The specific biovolume values calculated were significantly higher for the PAC than the control reactor ($\sim 24 \mu\text{m}^3/\mu\text{m}^2$ vs. $\sim 12 \mu\text{m}^3/\mu\text{m}^2$). The elevation in biofilm growth, when PAC was supplemented, supports the higher reduction in membrane permeability, induced by the elevation of SMP component adsorption, which may provide better conditioning of the membrane surface, enhancing biofilm formation.

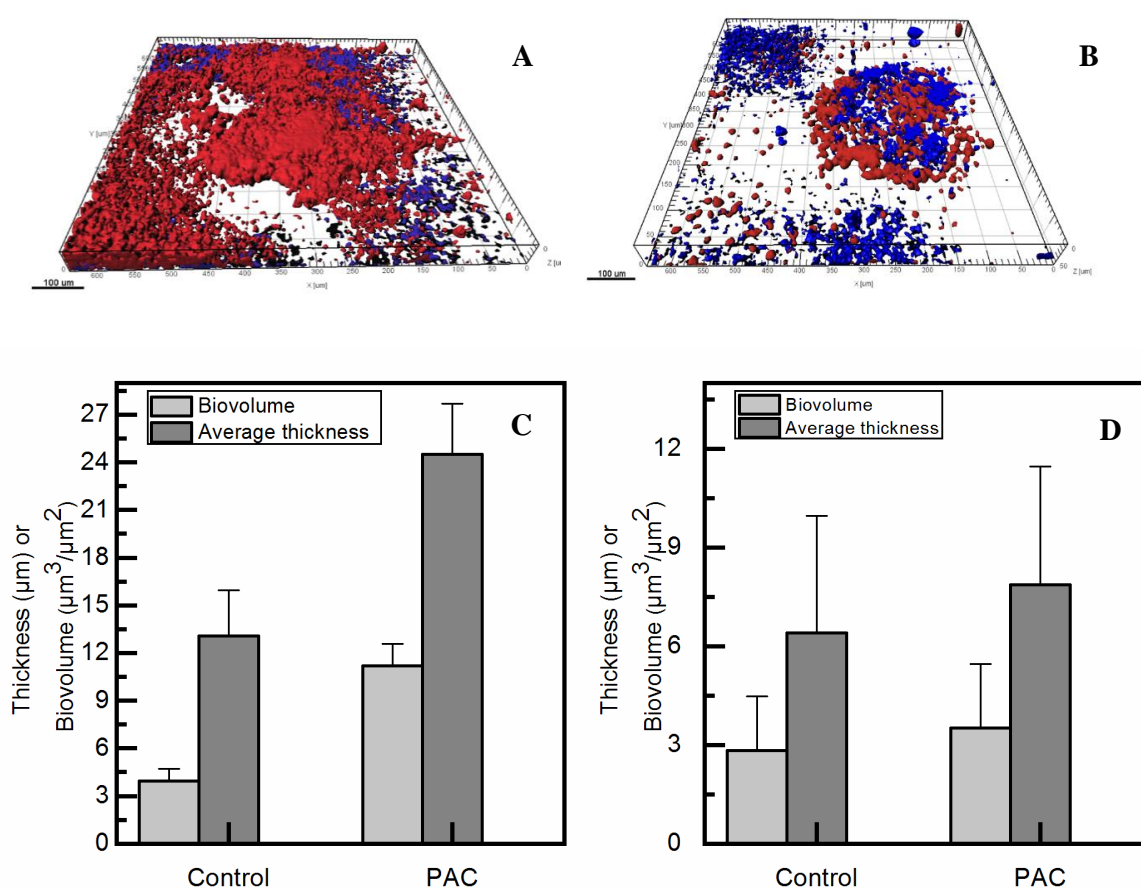


Figure 5. The effect of PAC addition to the MBRs on biofilm formation: Representative CLSM 3-D reconstructed images (red and blue spots are contributed by dead cells and extracellular polymeric substances (EPS), respectively) of the biofilms on the UF membrane in the MBRs with and w/o PAC. Images (A) and (B) are $635 \mu\text{m} \times 635 \mu\text{m}$ and the scale bar represents $100 \mu\text{m}$. Plots (C) and (D) provide the calculated biovolume and thickness of the fixed cells and EPS, respectively, in the MBRs' biofilm.

Since the greater decrease in membrane permeability in the MBR supplemented with PAC could be potentially attributed to PAC particles, SEM imaging of the fouled membrane was carried out at the end of the first experiment (Figure 6 and Figure S3 in the SI). No major differences in the biofilm morphology of the membranes from the PAC and the control reactors were observed, and in both cases, embedded cells in the EPS matrix were detected. Notably, PAC particles were not recognized in any of

the samples collected from the PAC-supplemented reactor (Figure 6c,d and Figure S3 in the SI). Hence, the elevated TMP and higher decrease in the permeability of the membrane in the PAC reactors could not be attributed to a physical blockage of the membrane by PAC particles.

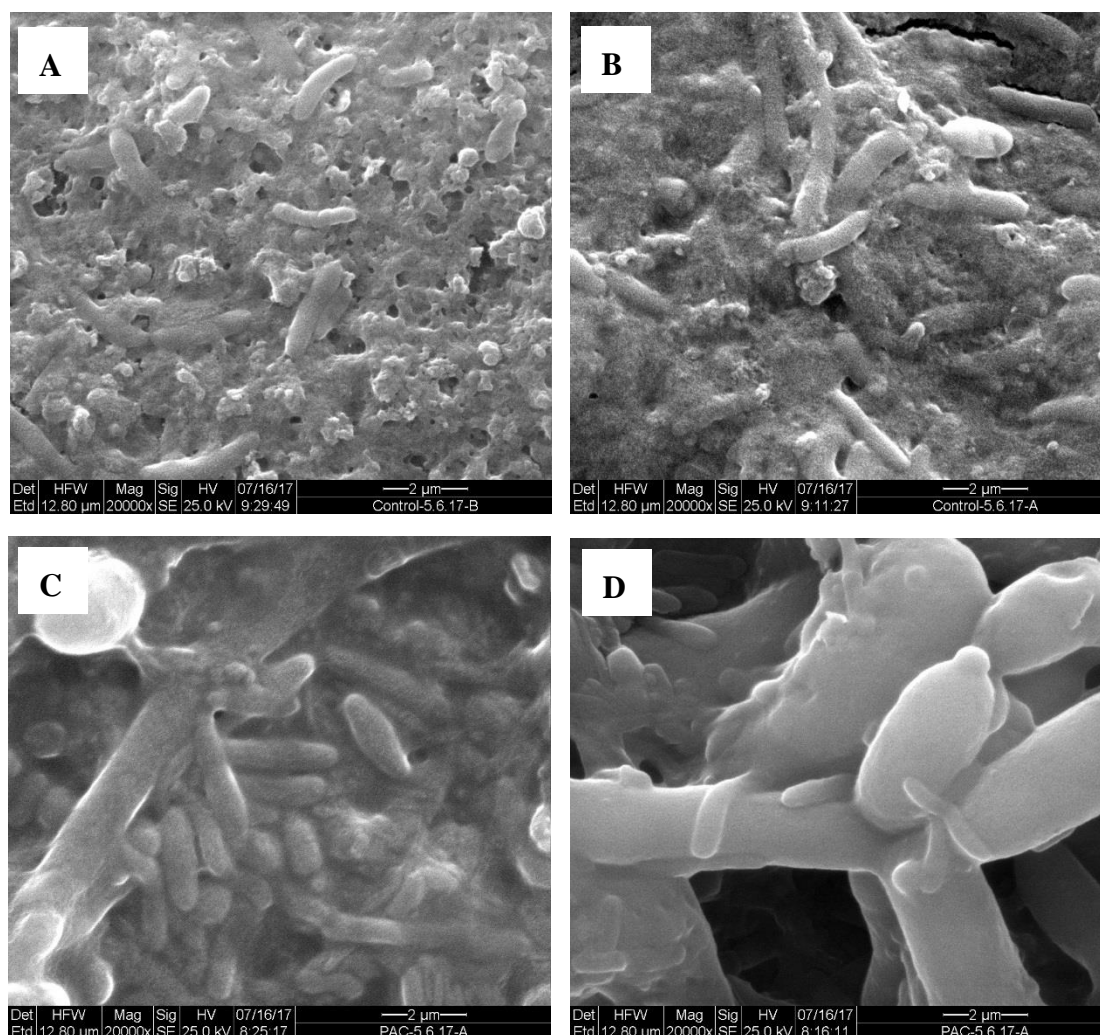


Figure 6. SEM imaging of the fouled membranes at the end of the first MBR experiment: Membrane autopsies from the MBRs with ((C) and (D)) and without ((A) and (B)) PAC.

4. Concluding Remarks

The effect of continuous PAC supplement to the MBR's MLSS on membrane fouling was tested for the case of OMWW treatment. Surprisingly, the results showed a negative effect of PAC addition on membrane performance. To the best of our knowledge, this is one of the first reports showing an increase in membrane fouling due to the addition of PAC to MBR system. The presence of PAC in the MLSS induced membrane fouling, causing a faster increase in the TMP and a decrease in the membrane permeability. PAC addition had almost no effect on the DOC and BOD concentrations of the MBR. However, addition of PAC elevated biomass activity and in parallel, the molecular weight distribution of the organic molecules in the reactors was altered as observed with GPC (fractions of 580–790 kDa organic molecules and organic molecules that are bigger than 4×10^3 kDa were elevated and reduced, respectively). The adsorption of the MBRs' SMP organic molecules to a membrane mimetic surface was tested using PES-coated QCM-D sensors. A significantly elevated adsorption of the dissolved organic sample originating from the SMP of the PAC-supplemented MBR was observed. Notably, the exposure of the MLSS in the MBR to PAC was likely the main reason for the elevated decline in

membrane permeability as observed in separated dead-end filtration experiments with SMP collected from the MBRs. Hence, the increased fouling in the presence of PAC was most likely the result of the elevated absorbance of a certain fraction of the organic molecules in the MBR, observed at a higher quantity with GPC in the molecular weight range of 580–790 kDa. Finally, CLSM biofilm formation on the different membranes showed a higher amount of biofilm on the membrane taken from the PAC reactor, with no traces of PAC particles observed when analyzed with SEM. In sum, altering the composition of the dissolved organic matter in the MBR with PAC promoted its adhesion to the membrane, induced biofilm formation, and more prominently, decreased membrane permeability.

Supplementary Materials: The following are available online at <http://www.mdpi.com/2073-4441/11/12/2498/s1>, Figure S1: Flux decline during fouling with SMP (50 ± 3 mg/L TOC dissolved in DI water) and corresponding irreversible permeability loss after 60 minutes filtration of SMP solution originated from the two MBR with and without PAC; Figure S2: The effect of PAC addition to the MBRs on the adherence properties of the EPS: QCM-D adhesion profiles of the EPS provided as frequency shifts during EPS adhesion to PES-coated sensors at the ninth overtone and a flow rate of 100 $\mu\text{l}/\text{min}$ of the EPS solution. A background solution with an ionic strength of 20 mM (17 mM NaCl \pm 1 mM CaCl₂) was supplemented with EPS (20 mg/l as DOC) extracted from the MLSS of the two runs (top and bottom panels correspond to panels a & b in Figure 3 of the original paper); Figure S3: SEM images of the biofilm layers developed on membranes taken from the two MBR systems, with and without PAC; Figure S4: Schematic diagram of the MBR; Figure S5: Permeability of the membranes in MBR-PAC and the control (w/o PAC) during the preliminary experiment. A rapid decline in the permeability of the membrane in the PAC reactor was observed versus slower decline in membrane permeability in the control reactor. Therefore, a gradual reduction in PAC concentration was performed. Once the PAC concentration in the reactor had reached the final concentration of 0.1 g/l, the permeability was close in the two reactors.

Author Contributions: Conceptualization, M.H. and J.G.; methodology, R.S.-G.; software, R.S.-G.; formal analysis, N.R.; investigation, N.R. M.H., and J.G.; writing—original draft preparation, N.R.; writing—review and editing, M.H. and J.G.; visualization, N.R.; supervision, M.H.; project administration, M.H. and J.G.; funding acquisition, M.H.

Funding: This research was funded by the Israel Ministry of Science, Technology and Space: Infrastructure Research in the Field of Engineering Science.

Conflicts of Interest: The authors declare no conflict of interest.

References

1. Khan, S.J.; Visvanathan, C.; Jegatheesan, V. Effect of powdered activated carbon (PAC) and cationic polymer on biofouling mitigation in hybrid MBRs. *Bioresour. Technol.* **2012**, *113*, 165–168. [[CrossRef](#)]
2. Le-Clech, P.; Chen, V.; Fane, T.A.G. Fouling in membrane bioreactors used in wastewater treatment. *J. Membr. Sci.* **2006**, *284*, 17–53. [[CrossRef](#)]
3. Gander, M.; Jefferson, B.; Judd, S. Aerobic MBRs for domestic wastewater treatment: A review with cost considerations. *Sep. Purif. Technol.* **2000**, *18*, 119–130. [[CrossRef](#)]
4. Judd, S. *The MBR Book: Principles and Applications of Membrane Bioreactors for Water and Wastewater Treatment*; Elsevier: Amsterdam, The Netherlands, 2010.
5. Guo, W.; Ngo, H.H.; Li, J. A mini-review on membrane fouling. *Bioresour. Technol.* **2012**, *122*, 27–34. [[CrossRef](#)] [[PubMed](#)]
6. Hall-Stoodley, L.; Costerton, J.W.; Stoodley, P. Bacterial biofilms: From the natural environment to infectious diseases. *Nat. Rev. Microbiol.* **2004**, *2*, 95. [[CrossRef](#)]
7. Liao, B.; Bagley, D.; Kraemer, H.; Leppard, G.; Liss, S. A review of biofouling and its control in membrane separation bioreactors. *Water Environ. Res.* **2004**, *76*, 425–436. [[CrossRef](#)]
8. Herzberg, M.; Dosoretz, C.G.; Tarre, S.; Green, M. Patchy biofilm coverage can explain the potential advantage of BGAC reactors. *Environ. Sci. Technol.* **2003**, *37*, 4274–4280. [[CrossRef](#)]
9. Herzberg, M.; Dosoretz, C.G.; Tarre, S.; Michael, B.; Dror, M.; Green, M. Simultaneous removal of atrazine and nitrate using a biological granulated activated carbon (BGAC) reactor. *J. Chem. Technol. Biotechnol. Int. Res. Process Environ. Clean Technol.* **2004**, *79*, 626–631. [[CrossRef](#)]
10. Satyawali, Y.; Balakrishnan, M. Effect of PAC addition on sludge properties in an MBR treating high strength wastewater. *Water Res.* **2009**, *43*, 1577–1588. [[CrossRef](#)]

11. Skouteris, G.; Saroj, D.; Melidis, P.; Hai, F.I.; Ouki, S. The effect of activated carbon addition on membrane bioreactor processes for wastewater treatment and reclamation—A critical review. *Bioresour. Technol.* **2015**, *185*, 399–410. [[CrossRef](#)]
12. Goswami, L.; Kumar, R.V.; Borah, S.N.; Manikandan, N.A.; Pakshirajan, K.; Pugazhenth, G. Membrane bioreactor and integrated membrane bioreactor systems for micropollutant removal from wastewater: A review. *J. Water Process Eng.* **2018**, *26*, 314–328. [[CrossRef](#)]
13. Ceconet, D.; Molognoni, D.; Callegari, A.; Capodaglio, A. Biological combination processes for efficient removal of pharmaceutically active compounds from wastewater: A review and future perspectives. *J. Environ. Chem. Eng.* **2017**, *5*, 3590–3603. [[CrossRef](#)]
14. Li, Y.Z.; He, Y.L.; Liu, Y.H.; Yang, S.C.; Zhang, G.J. Comparison of the filtration characteristics between biological powdered activated carbon sludge and activated sludge in submerged membrane bioreactors. *Desalination* **2005**, *174*, 305–314. [[CrossRef](#)]
15. Ying, Z.; Ping, G. Effect of powdered activated carbon dosage on retarding membrane fouling in MBR. *Sep. Purif. Technol.* **2006**, *52*, 154–160. [[CrossRef](#)]
16. Johir, M.; Aryal, R.; Vigneswaran, S.; Kandasamy, J.; Grasmick, A. Influence of supporting media in suspension on membrane fouling reduction in submerged membrane bioreactor (SMBR). *J. Membr. Sci.* **2011**, *374*, 121–128. [[CrossRef](#)]
17. Zhang, S.; Xiong, J.; Zuo, X.; Liao, W.; Ma, C.; He, J.; Chen, Z. Characteristics of the sludge filterability and microbial composition in PAC hybrid MBR: Effect of PAC replenishment ratio. *Biochem. Eng. J.* **2019**, *145*, 10–17. [[CrossRef](#)]
18. Zouboulis, A.; Gkotsis, P.; Zamboulis, D.; Mitrakas, M. Application of powdered activated carbon (PAC) for membrane fouling control in a pilot-scale MBR system. *Water Sci. Technol.* **2017**, *75*, 2350–2357. [[CrossRef](#)]
19. Ng, C.A.; Sun, D.; Zhang, J.; Wu, B.; Fane, A.G. Mechanisms of fouling control in membrane bioreactors by the addition of powdered activated carbon. *Sep. Sci. Technol.* **2010**, *45*, 873–889. [[CrossRef](#)]
20. Al-Malah, K.; Azzam, M.O.; Abu-Lail, N.I. Olive mills effluent (OME) wastewater post-treatment using activated clay. *Sep. Purif. Technol.* **2000**, *20*, 225–234. [[CrossRef](#)]
21. Niaounakis, M.; Halvadakis, C.P. *Olive Processing Waste Management: Literature Review and Patent Survey*; Elsevier: Amsterdam, The Netherlands, 2006.
22. Miccio, M.; Poletto, M. Disposal of olive mill waste waters through concentration and combustion: Comparison between different process options. *Chem. Eng. Trans.* **2009**, *17*, 221–226.
23. Aktas, E.S.; Imre, S.; Ersoy, L. Characterization and lime treatment of olive mill wastewater. *Water Res.* **2001**, *35*, 2336–2340. [[CrossRef](#)]
24. Rivas, F.J.; Beltrán, F.J.; Gimeno, O.; Frades, J. Treatment of olive oil mill wastewater by Fenton's reagent. *J. Agric. Food Chem.* **2001**, *49*, 1873–1880. [[CrossRef](#)] [[PubMed](#)]
25. Inan, H.; Dimoglo, A.; Şimşek, H.; Karpuzcu, M. Olive oil mill wastewater treatment by means of electro-coagulation. *Sep. Purif. Technol.* **2004**, *36*, 23–31. [[CrossRef](#)]
26. Adhoum, N.; Monser, L. Decolourization and removal of phenolic compounds from olive mill wastewater by electrocoagulation. *Chem. Eng. Process. Process Intensif.* **2004**, *43*, 1281–1287. [[CrossRef](#)]
27. Tsioulpas, A.; Dimou, D.; Iconomou, D.; Aggelis, G. Phenolic removal in olive oil mill wastewater by strains of *Pleurotus* spp. in respect to their phenol oxidase (laccase) activity. *Bioresour. Technol.* **2002**, *84*, 251–257. [[CrossRef](#)]
28. Hamdi, M. Toxicity and biodegradability of olive mill wastewaters in batch anaerobic digestion. *Appl. Biochem. Biotechnol.* **1992**, *37*, 155–163. [[CrossRef](#)]
29. Eroğlu, E.; Eroğlu, İ.; Gündüz, U.; Türker, L.; Yücel, M. Biological hydrogen production from olive mill wastewater with two-stage processes. *Int. J. Hydrog. Energy* **2006**, *31*, 1527–1535. [[CrossRef](#)]
30. Pulido, J.M.O. A review on the use of membrane technology and fouling control for olive mill wastewater treatment. *Sci. Total Environ.* **2016**, *563*, 664–675. [[CrossRef](#)]
31. Stoller, M.; Bravi, M.; Chianese, A. Threshold flux measurements of a nanofiltration membrane module by critical flux data conversion. *Desalination* **2013**, *315*, 142–148. [[CrossRef](#)]
32. Ioannou-Ttofa, L.; Michael-Kordatou, I.; Fattas, S.; Eusebio, A.; Ribeiro, B.; Rusan, M.; Amer, A.; Zuraiqi, S.; Waismand, M.; Linder, C. Treatment efficiency and economic feasibility of biological oxidation, membrane filtration and separation processes, and advanced oxidation for the purification and valorization of olive mill wastewater. *Water Res.* **2017**, *114*, 1–13. [[CrossRef](#)]

33. Paraskeva, C.; Papadakis, V.; Tsarouchi, E.; Kanellopoulou, D.; Koutsoukos, P. Membrane processing for olive mill wastewater fractionation. *Desalination* **2007**, *213*, 218–229. [[CrossRef](#)]
34. Fazal, S.; Zhang, B.; Zhong, Z.; Gao, L.; Chen, X. Industrial wastewater treatment by using MBR (membrane bioreactor) review study. *J. Environ. Prot.* **2015**, *6*, 584. [[CrossRef](#)]
35. Dhaouadi, H.; Marrot, B. Olive mill wastewater treatment in a membrane bioreactor: Process feasibility and performances. *Chem. Eng. J.* **2008**, *145*, 225–231. [[CrossRef](#)]
36. Wang, X.; Ruengruglikit, C.; Wang, Y.-W.; Huang, Q. Interfacial interactions of pectin with bovine serum albumin studied by quartz crystal microbalance with dissipation monitoring: Effect of ionic strength. *J. Agric. Food Chem.* **2007**, *55*, 10425–10431. [[CrossRef](#)] [[PubMed](#)]
37. Heydorn, A.; Nielsen, A.T.; Hentzer, M.; Sternberg, C.; Givskov, M.; Ersbøll, B.K.; Molin, S. Quantification of biofilm structures by the novel computer program COMSTAT. *Microbiology* **2000**, *146*, 2395–2407. [[CrossRef](#)] [[PubMed](#)]
38. Sweity, A.; Zere, T.R.; David, I.; Bason, S.; Oren, Y.; Ronen, Z.; Herzberg, M. Side effects of antiscalants on biofouling of reverse osmosis membranes in brackish water desalination. *J. Membr. Sci.* **2015**, *481*, 172–187. [[CrossRef](#)]



© 2019 by the authors. Licensee MDPI, Basel, Switzerland. This article is an open access article distributed under the terms and conditions of the Creative Commons Attribution (CC BY) license (<http://creativecommons.org/licenses/by/4.0/>).